Preferential orientation and anomalous interfacial tensions in aqueous solutions of alcohols

Jesús Algaba,[†] José Manuel Míguez,[†] Paula Gómez-Álvarez,[†] Andrés Mejía,[‡] and Felipe J. Blas[*,†]

[†]*Laboratorio de Simulación Molecular y Química Computacional, CIQSO-Centro de Investigación en Química Sostenible and Departamento de Ciencias Integradas, Universidad de Huelva, 21006 Huelva, Spain*

[‡]*Departamento de Ingeniería Química, Universidad de Concepción, POB 160-C Concepción, Chile*

E-mail: felipe@uhu.es

Phone: +34 959219796. Fax: +34 959219777

Abstract

Literature studies regarding the interfacial tension versus temperature between normal alcohols and water show that it increases with temperature and exhibits a maximum value at a given temperature depending on the molecular weight of the alcohol. This very unusual behavior is supposedly accompanied by the formation of monolayers of alcohol molecules oriented preferentially at the interface, a structural issue not confirmed until now. We use molecular-based models for water and alcohols in combination with molecular dynamics simulation to provide physical insights, from a molecular perspective, of the structural and thermodynamic behavior at the liquid-liquid interface of aqueous solutions of alcohols.

Introduction

When two different liquids are mixed, chemical characteristics of both components and their affinities, at a given temperature and pressure, determine if the system is thermodynamically stable and forms a single-stable phase, or contrary, separates spontaneously into two liquids immiscible phases. Liquid-liquid (LL) immiscibility is an amazing phenomenon that can be explained as a competition between energetic (enthalpic) and entropic effects.[1] The energetic contribution to the free energy of the system is determined by intermolecular interactions. Forces between molecules of the same species are usually stronger than those between different components of the mixture. Consequently, the enthalpic contribution to free energy becomes positive and the system eventually tends to demix. However, this is a part of the story. Mixing of liquids produces a huge increase of compositional and orientational entropy, which contributes to decrease the free energy of the system at high temperatures. The competition between energetic (interactions) and entropic (mixing) contributions underlies the formation of a single miscible phase or two immiscible phases. Usually, extend separation decreases as temperature is increased, and the immiscibility disappears above the so-called upper critical solution temperature (UCST) as the unfavourable interactions between unlike

molecules are overcome by the compositional and orientational increase of entropy.[1]

The precise knowledge of phase behaviour of mixtures that exhibit LL immiscibility is essential in many scientific and engineering fields.[2–4] During last years, however, there have been an increasing interest in a detailed knowledge, from a molecular perspective, of structural and intrinsic properties associated to LL interfaces, with special emphasis on intrinsic density profiles which provide a route to obtain a truly description on the structure of interfacial region on LL interfaces. For a complete description and methodological approach, the reader is redirected to the Bresme *et al.*[5] work and references therein. This interest is not only ascribed to theoretical fields but also to an important number of applied disciplines. The accurate knowledge of interfacial concentrations, interfacial thickness, and interfacial tension, as well as surface activity, among others, is key for controlling many processes and their efficiencies in different fields, including chemical, petroleum, and environmental engineering. Liquid extraction, interfacial chemical reactions, emulsification of liquids, phase wettability, capillary pressure, and relative permeability, among others, are only a few examples of processes and phenomena in which an accurate knowledge of structural properties, and especially interfacial tension, are required to find efficiently solutions in different areas, such as tertiary oil recovery and gas injection in enhanced oil recovery technologies[6–8] or contaminants removal in aquifers and for groundwater remediation.[9]

Aqueous solutions of alcohols constitute an interesting example of systems that exhibit LL immiscibility.[1] The first members of the homologous series, from methanol up to propan-1-ol, are completely miscible (only vapour-liquid phase separation exists in these systems). However, from the butan-1-ol + water, the mixtures exhibit regions of LL immiscibility below the corresponding UCSTs due to the enhancement of unfavourable energetic contribution against the loss of entropy.[1] Although in most cases LL immiscibility is enhanced as the temperature decreases, in this case immiscibility disappears if temperature is further lowered at a lower critical solution temperature (LCST). This behavior, due to the presence of unlike butan-1-ol – water hydrogen bonding that overcomes any other unfavourable effect, produces

the so-called closed-loop immiscibility and the corresponding reentrant miscibility.[10–13] It is interesting to note that the global phase equilibrium of the butan-1-ol + water binary mixture exhibits type VI phase behavior according to the classification of Scott and Konynenburg.[14,15] According to this, the type VI binary mixtures are characterized by two critical lines and a heteroazeotropic line. One of the two critical lines is a continuum critical line connecting their pure components critical points. In this region, the all subcritical phase equilibria are characterized by a completely miscible liquid phase in every temperature condition. This fact implies that all subcritical states of this zone exhibit only vapor-liquid equilibria. The second critical line appears at the low temperature range and comes from a lower critical end point (LCEP) to an upper critical end point (UCEP). This critical line is a liquid-liquid critical line having a pressure maximum. In this region, the subcritical phase equilibria are characterized liquid–liquid closed-loop immiscibility. Finally, the heteroazeotropic line connects both CEPs and it is characterized by a vapor-liquid-liquid equilibrium. Specific aspects relate to type VI, its construction as well as the prediction of its subcritical phase equilibrium have been extensively described by Rowlinson and Swinton[1] and Deiters and Kraska.[16] However, the LCST of the mixture is not present at low pressures since is located inside the solid boundaries of the system.[12,13] Although the phenomenon of closed-loop immiscibility has been of long-standing interest since Hirschfelder and co-workers[17] proposed in 1937 that directional forces (hydrogen bonding) are the direct cause of the existence of an LCST, and it is common in a large number of mixtures,[1,18–25] perhaps the most interesting and nearly unique feature of the alcohol + water systems is the unusual behaviour of the LL interfacial tension of this homologous series.

Despite the simplicity of aqueous solutions of primary linear alcohols, the LL interfacial tension of these mixtures exhibits a number of unusual features that make these systems very interesting from a theoretical point of view, and particularly from a molecular perspective. On the one hand, the interfacial tension increases with temperature at low temperatures, it shows a parabolic shape as a function of temperature, contrary to what happens with

most aqueous solutions of organic compounds. On the other hand, it exhibits low interfacial energy values compared with similar systems that do not interact through specific interactions (hydrogen bonding), such as mixtures of water with alkanes with nearly the same molecular weight and structure (with the exception of the alcohol chemical group).[26–29] This phenomenon is unusual in nature and, from our knowledge, only the interfacial tension of a few systems exhibit these characteristics and apparent counterintuitive behaviour: aqueous solutions of alcohols,[26–28] mixtures of fatty acids methyl esters with water,[30] and mixtures of 1-butyl-3-methylimidazolium thiocyante or [BMIM][SCN] ionic liquid with linear alcohols (butan-1-ol, pentan-1-ol, and hexan-1-ol)[31] and 1-ethyl-3-methylimidazolium ethyl sulfate or 1-butyl-3-methylimidazolium hexafluorophosphate with carbon dioxide.[32]

From a thermodynamic perspective, the variation of the LL interfacial tension with temperature is directly related with the mutual solubilities of the immiscible liquids. Clearly, cohesional forces of molecules in LL systems determine, not only the magnitude of the interfacial tension but also the extent to which a given compound is soluble in a particular solvent. Following this idea, Donahue and Bartell[33] proposed a linear relation between the LL interfacial tension of aqueous solutions of organic liquids and the logarithm of the "degree of immiscibility" $n_1 + n_2$, being n_1 the molar fraction of the organic compound in the aqueous liquid phase and n_2 the molar fraction of water in the organic liquid phase. They used this relationship to correlate more than 30 organic liquids and show that interfacial tension, at constant temperature, decreases as the degree of miscibility increases. In other words, the temperature coefficient of the interfacial tension (variation of interfacial tension with temperature at constant pressure) or simply surface entropy, is directly related with the temperature coefficient of the miscibility. According to Donahue and Bartell,[33] most of the systems considered exhibit positive surface entropy values, which means that interfacial tension should decrease with temperature. Indeed, this is the classical situation in which interfacial tension decreases with temperature as the system approaches to the UCTS, point of the phase diagram at which miscibility of both liquids is complete. These authors cited

the work of Ssementschenko and co-workers[34] who found that the interfacial tension of the nicotine + water mixture increases as the temperature is raised in the region in which the temperature coefficient of miscibility is highly negative. This system exhibits type VI phase behavior following the classification of Scott and van Konynenburg.[14,15] According to this, at the lowest temperatures of the closed-loop of immiscibility, the mutual miscibilities of nicotine and water decrease with temperature, following the hypothesis of Donahue and Bartell.[33] Interestingly, the same qualitative behavior is observed in the aqueous solutions of butan-1-ol.[10–13]

Thirty-five years later, Villers and Platten[26] measured and analyzed carefully the temperature dependence of the interfacial tension of aqueous solutions of long-chain alcohols (up to dodecan-1-ol). According to their nice results, the interfacial tension increases with the number of carbon atoms in the alcohols and all interfacial tension curves show parabolic profiles. Following the seminal work of Donahue and Bartell,[33] these results are interpreted in terms of mutual solubilities of water and linear alcohols. Since solubilities present minima with the temperature, it is not surprising that interfacial tensions also exhibit maxima with temperature. Tian *et al.*[27] and Ghatee and Ghazipour[28] have also confirmed these results studying the interfacial tension of some aqueous mixtures of organic compounds, including alcohols, alkanes, and hexanoic acid.

Most of the studies devoted to the analysis of aqueous organic mixtures suggest that the polar groups of alcohols (–OH) and carboxylic acids (–COOH) of the organic molecules should be capable of attaching to the surface of the water-rich phase and form an oriented monolayer over the water surface, with the hydrophobic end alkyl groups towards the organic-rich liquid phase.[33] This behavior should be consistent with the substantially lower interfacial tension of aqueous mixtures of alcohols and carboxylic acids in comparison with mixtures of alkanes.[27,28] It is interesting to note that this behavior is consistent with the structural organization of surfactants in aqueous - organic interfaces. Non-ionic surfactant alkyl polyoxyethylens ethers, which can be represented by the general formula C_iE_j

or $H(CH_2)_i(OCH_2CH_2)_jOH$, exhibit complex organized structures, including surfactant micelles and lyotropic liquid crystalline phases, as cubic, hexatic, and lamellar structures, as well as closed-loop immiscibility regions.[12,13] In fact, primary linear alcohols can be considered as primitive surfactants and members of the C_iE_j surfactants with the formula C_nE_0. The nature of interactions between alcohol and water molecules is in general understood from a molecular perspective, i.e., favourable interactions mediated by specific OH - H_2O hydrogen bondings (highly directional) and unfavourable water - alkyl groups interactions. The exact orientation of both species at the interface has been described for the case of octan-1-ol + water[35,36] and hexan-1-ol + water,[37] where it is possible to conclude that strong orientational preference is observed for the hydrogen-bonded alcohol molecules at the interface. Apart from these studies, there is no a systematic microscopic study for aqueous solutions of alcohols with different molecular weights on the formation of an oriented monolayer over the water surface, as argued by Donahue and Bartell,[33] neither precise information on how the alcohols molecules adopt a preferential orientation with the hydrophilic ends pointing towards the aqueous phase and the alkyl chains across the interface, as stated by Ghatee and Ghazipour[28] as a function of the molecular weight of alcohols.

The aim of this contribution is twofold; we use molecular simulation to understand, from a microscopic point of view, how primary linear alcohols and water molecules are distributed across the LL interface of aqueous solutions of alcohols, with particular emphasis on the formation of layers of organic compounds oriented preferentially at the interface. Also, and taking advantage of the same microscopic models, we show how molecular-based tools can provide physical insights into the unusual behavior of the interfacial tension between long-chain alcohols and water at both the macroscopic and molecular level.

The rest of the paper is organized as follows. In Sections 2 and 3 we summarize the molecular models used to predict the interfacial behavior of aqueous solutions of linear primary alcohols and computer simulation details, respectively. We discuss the results obtained in Section 4. Finally, the conclusions and presented in the last Section.

Models

In this work, water molecules are described using the well-known TIP4P/2005 water model proposed by Abascal and Vega.[38] It is a non-polarizable model that considers four interacting sites placed on the three atom positions (one for the oxygen atom, O, and two for the hydrogen atoms, H) and an additional site placed in the bisector of the angle formed by the molecule bonds (I). This model provides very accurate estimates of water bulk properties, in comparison with the most common models of water, such as SPC, SPC/E, TIP3P, TIP4P, TIP4P/Ew, and TIP5P, but also is remarkably proficient in the estimation of interfacial properties.[39,40] Linear alcohols are modeled using the TraPPE-UA (transferable potentials for phase equilibria united-atoms) models of Chen *et al.*[41]

The nonbonded interactions between chemical groups separated by more than three bonds are described by the Lennard-Jones and Coulomb intermolecular potentials

$$U(r_{ij}) = 4\epsilon_{ij}\left[\left(\frac{\sigma_{ij}}{r_{ij}}\right)^{12} - \left(\frac{\sigma_{ij}}{r_{ij}}\right)^{6}\right] + \frac{q_i q_j}{4\pi\epsilon_0 r_{ij}} \tag{1}$$

where r_{ij} is the distance between interacting sites i and j, σ_{ij} and ϵ_{ij} are the diameter and well depth associated to the LJ intermolecular potential, q_i and q_j are the partial charges on interacting sites i and j, and ϵ_0 the permittivity of vacuum. The molecular parameters used in this work to describe the nonbonded interactions, including partial charges values for electrostatic interactions, are summarized in Table 1. All the LJ parameters for unlike interactions are obtained using the Lorentz-Berthelot combining rules.

The values of the fixed bond lengths, that are taken from the original works of Abascal and Vega[38] and Chen *et al.*,[41] are also shown in Table 2. The bending and torsional force field parameters corresponding to the bonded interactions for the linear alcohols are obtained from the TraPPE-UA force fields.[41] The bond bending potential is controlled through a harmonic function

Table 1: Lennard-Jones well depth, ϵ, size, σ, and partial charges, q, parameters for the TIP4P/2005 and TraPPE-UA force fields corresponding to the non-bonded interactions of water and linear alcohols, respectively. In the case of linear alcohols, the letters in parenthesis indicate the atom a particular site is bonded to. All values are taken from the works of Abascal and Vega[38] and Chen *et al.*[41]

atom	ϵ/k_B(K)	σ(Å)	q(e)
H_2O (TIP4P/2005)			
O	93.0	3.1589	0.0000
H	00.0	0.0000	0.5564
I	00.0	0.0000	-1.1128
linear alcohols (TraPPE-UA)			
CH_3–(CH_x)	98.0	3.7500	0.0000
(CH_x)–**CH_2**–(CH_y)	46.0	3.9500	0.0000
(CH_x)–**CH_2**–(O)–(H)	46.0	3.9500	0.2650
(CH_x)–**O**–(H)	93.0	3.0200	-0.7000
(O)–**H**	00.0	0.0000	0.43500

$$U_{bend}(\theta) = \frac{1}{2} k_\theta (\theta - \theta_0)^2 \tag{2}$$

where θ, θ_0, and k_θ are the measured bending angle, the equilibrium bending angle, and the force constant, respectively. Table 3 contains the list of the θ_0, and k_θ values used in this work as proposed by Chen *et al.*[41] According to the philosophy of the TraPPE-UA force field approach, the dihedral rotations around bonds connecting four chemical groups are account for the standard cosine series of the dihedral angle

$$U_{tor} = c_0 + c_1[1 + \cos(\phi)] + c_2[1 + \cos(2\phi)] + c_3[1 + \cos(3\phi)] \tag{3}$$

where the Fourier coefficients $\{c_i\}$, for $i = 0, \ldots, 3$ are listed in Table 4.

Simulation details

All the properties of interest have been obtained combining molecular dynamics (MD) computer simulations and the direct coexistence technique. To study liquid-liquid (LL) interfacial

Table 2: Bond length values of the TIP4P/2005 and TraPPE-UA force fields corresponding to water and linear alcohols, respectively. Values are taken from the works of Abascal and Vega[38] and Chen *et al.*[41]

bond	bond length (Å)
H_2O (TIP4P/2005)	
O–H	0.9572
O–I	0.1546
linear alcohols (TraPPE-UA)	
CH_x–CH$-y$	1.540
CH_x–OH	1.430
O–H	0.945

Table 3: Bending potential parameters for the TraPPE-UA force field corresponding to linear alcohols All values are taken from the work of Chen *et al.*[41]

bending	θ (deg)	k_θ/k_B (K/rad^2)
CH_x–$\mathbf{CH_2}$–CH_y	114.0	62500
CH_x–$\mathbf{CH_y}$–OH	109.5	50400
O–H	108.5	55400

Table 4: Torsional potential parameters for the TraPPE-UA force field corresponding to linear alcohols. All values are taken from the work of Chen *et al.*[41]

torsion	c_0/k_B (K)	c_1/k_B (K)	c_2/k_B (K)	c_3/k_B (K)
CH_x–CH_2–CH_2–CH_y	0.00	355.03	-68.19	791.32
CH_x–CH_2–CH_2–O	0.00	176.62	-53.34	769.93
CH_x–CH_2–O–H	0.00	209.82	-29.17	187.93

properties of the mixtures considered here we have used the isothermal-isobaric or $NP_z\mathcal{A}T$ ensemble to ensure that temperature and pressure are constants. During the simulations the interfacial area $\mathcal{A} = L_x \times L_y$ is kept constant and only L_z is varied along the simulation. Here L_x, L_y, and L_z are the dimensions of the simulation box along x, y and z axis, respectively. For convenience, the z-axis is chosen perpendicular to the planar interfacial or parallel to the direction along which the system exhibits the LL inhomogeneity. We use periodic boundary conditions.

Previous to the construction of the box to simulate the LL interface, two bulk liquid systems, one corresponding to the organic-rich phase and other to the water-rich phase, are equilibrated independently using simulation boxes with the same L_x and L_y, but different L_z depending on the system and thermodynamic conditions. The size of the initial bulk simulation boxes are prepared using as initial values for density and composition the experimental data taken from the literature at the same temperature.[29,42] Both phases are equilibrated at the same pressure and temperature using the $NP_z\mathcal{A}T$ isothermal-isobaric ensemble to ensure that L_x and L_y do not vary. All computer simulations have been performed at atmospheric pressure (1 bar), and temperatures ranging from 280 up to 380 K for all the aqueous mixtures considered from butan-1-ol to heptan-1-ol. Since we are studying binary mixtures, the composition of the system varies with the temperature. In order to keep constant the total number of molecules for all the systems and temperatures considered, we have used different simulation box lengths along the z-axis. According to this, the dimensions of the homogeneous water-rich and organic-rich simulation boxes are $L_x = L_y = 4$ nm and we use different values of L_z depending on the system and temperature studied. In all cases, we consider 2200 water molecules in the bulk aqueous simulation box (without alcohol molecules) and 1400 water and alcohol molecules in the bulk organic-rich simulation box. The particular number of water and alcohol molecules in the organic-rich simulation box depends on the mixture and temperature considered. For example, for the pentan-1-ol + water binary mixture, we use 490 water molecules and 910 pentan-1-ol molecules at 280 K, but 700 water

molecules and 700 pentan-1-ol molecules at 380 K. However, since the alcohol composition at the organic-rich phase increases as the molecular weight of the alcohol increases according to experimental data taken from the literature,[42] we use 350 water molecules and 1050 heptan-1-ol molecules at 280 K, and 520 and 880 water and heptan-1-ol molecules, respectively, at 380 K in the case of the heptan-1-ol + water binary mixture.

The interfacial simulation box is then constructed linking up three homogeneous simulation boxes, the bulk water-rich simulation box surrendered by two identical copies of the organic-rich box previously described. The simulation box contains then two LL interfacial regions, according to the standard methodology for simulating planar interfaces using the direct coexistence simulation technique.[43–48] The final overall dimensions of the interfacial simulation boxes (organic-rich + water-rich + organic-rich) are $L_x = L_y = 4\,\mathrm{nm}$ and L_z ranging from 20 to 40 nm depending on the particular system and temperature to be simulated. In particular, for the butan-1-ol + water mixture, $L_z = 20.6$ and 19.6 nm at 280 and 380 K, respectively. In the case of the longest organic molecules considered in this work, the heptan-1-ol + water binary mixture, $L_z = 36.5$ and 35 nm at 280 and 380 K, respectively. These configurations allow to simulate exactly the same number of molecules for all the mixtures (from butan-1-ol + heptan-1-ol + water), $N = 5000$. The detailed account for the number of molecules used during the simulations and the actual values of L_z are included in Table 5.

All MD computer simulations have been performed using the GROMACS software package (version 4.6.1).[49] In order to reduce the CPU time involved in the phase equilibrium and interfacial properties calculations, intermolecular interactions have been truncated at a cut-off radius (r_c) equal to a value of 1.975 nm. It has been shown by several authors[50–52] that such a value provides a reasonable description for the interfacial properties. Electrostatic interactions are obtained using the Ewald sums methods. The real part of the Coulombic potential is truncated at $r_c = 1.975\,\mathrm{nm}$. The Fourier term of the Ewald sums is evaluated using the particle mesh Ewald (PME) method. The width of the mesh is set equal to $1\,\mathrm{A}^{-1}$

Table 5: Number of water molecules, $N^{(\mathbf{O})}_{\mathbf{H_2O}}$, and alcohol molecules, $N^{(\mathbf{O})}_{\mathbf{COH}}$, used to simulate the initial organic-rich simulation box, and number of water molecules, $N^{(\mathbf{W})}_{\mathbf{H_2O}}$ used to simulate the initial water-rich simulation box. N is the total number of molecules used during the simulations of the LL interface. Note that $N = 2 \times \left(N^{(\mathbf{O})}_{\mathbf{H_2O}} + N^{(\mathbf{O})}_{\mathbf{COH}}\right) + N^{(\mathbf{W})}_{\mathbf{H_2O}}$ since we have two organic-rich simulation boxes surrounding the water-rich simulation box in order to form the interfacial simulation box. L_z denotes the final overall dimension of the interfacial simulation box along the z-axis (organic-rich + water-rich + organic-rich) for the alcohol + water mixtures considered in this work at different temperatures.

T (K)	$N^{(\mathrm{O})}_{\mathrm{H_2O}}$	$N^{(\mathrm{O})}_{\mathrm{COH}}$	$N^{(\mathrm{W})}_{\mathrm{H_2O}}$	N	L_z (nm)
butan-1-ol + water					
280	700	700	2200	5000	20.6
300	700	700	2200	5000	20.6
320	700	700	2200	5000	20.6
340	770	630	2200	5000	20.1
360	840	560	2200	5000	19.9
380	980	420	2200	5000	19.6
pentan-1-ol + water					
280	490	910	2200	5000	26.2
300	490	910	2200	5000	26.8
320	490	910	2200	5000	27.3
340	560	840	2200	5000	26.3
360	630	770	2200	5000	25.6
380	700	700	2200	5000	24.6
hexan-1-ol + water					
280	420	980	2200	5000	31.3
300	420	980	2200	5000	32.0
320	420	980	2200	5000	33.6
340	480	920	2200	5000	32.3
360	480	920	2200	5000	32.3
380	570	830	2200	5000	30.9
heptan-1-ol + water					
280	350	1050	2200	5000	36.5
300	350	1050	2200	5000	37.3
320	350	1050	2200	5000	38.0
340	430	970	2200	5000	36.6
360	430	970	2200	5000	37.5
380	520	880	2200	5000	35.0

and a maximum value for the reciprocal lattice equal to 31 is used.

We have used the Verlet leapfrog[53] algorithm with a time step of 0.001 ps. It is important to note that the time step value chosen has been necessary to sample correctly the torsional potentials of alcohols models. A Nosé-Hoover thermostat[54] with a time constant equal to 2.0 ps has been used to kept constant the temperature of the system. In addition to that, a Parrinello-Rahman barostat[55] with a relaxation time of 1 ps is also used to kept the pressure constant and equal to 1 bar. Simulations of the homogeneous liquid systems are equilibrated during 20 ns. After this, the alcohol-rich + water-rich + alcohol-rich systems are also equilibrated during 10 ns. After the systems reach equilibrium, the properties of the coexisting liquid phases are obtained as appropriate averages during 50 ns. In order to estimate errors on the variables computed, the sub-blocks average method has been applied.[56] In such approach, the production period is divided into M independent blocks. The statistical error is then deduced from the standard deviation of the average $\bar{\sigma}/\sqrt{M}$, where $\bar{\sigma}$ is the variance of the block averages and M has been fixed in this work to $M = 10$.

The equilibrium vapour pressure, P, and interfacial tension, γ, are obtained from the diagonal components of the pressure tensor. The vapour pressure corresponds to the normal component, $P \equiv P_{zz}$, of the pressure tensor, while the interfacial tension is obtained using the pressure route[57–60] as:

$$\gamma = \frac{L_z}{2}\left[\langle P_{zz}\rangle - \frac{\langle P_{xx}\rangle + \langle P_{yy})\rangle}{2}\right] \tag{4}$$

In Eq. (4), the additional factor 1/2 comes from having two interfaces in the system, and L_z is the size of the simulation box in the z direction, defined along the longitudinal dimension across the interface.

Results and discussion

In this section, we analyze the LL behavior of aqueous solutions of linear alcohols as obtained from $NP_z\mathcal{A}T$ MD in combination with the direct coexistence technique. This allows to account for structural and thermodynamic properties, including density profiles of species, coexistence densities and compositions, and interfacial tension from the evaluation of the tangential and normal components of the pressure tensor. Results obtained in this work for liquid densities, compositions, and interfacial tension as obtained from MD simulations are presented in Table 6.

Fig. 1 shows the density profiles of four alcohol + water mixtures at 1 bar and several temperatures as obtained from MD simulations. The equilibrium density profiles across the interface vary along the z-axis since the systems are inhomogeneous in that direction due to the LL immiscibility. The left size of the density profiles represent the alcohol-rich liquid phase and the right side the water-rich liquid phase. The bulk liquid density of the alcohols (in the organic-rich phases) decreases and that of water (in the organic-rich phases) increases as the temperature is raised. This is more noticeable in the case of alcohols than in water. In addition to that, the values of the alcohol density in the water-rich phase are nearly identical and lower than the water density in the organic-rich phase. This is a manifestation of the relatively low mutual solubilities of alcohols and water due to unfavourable forces between both components, particularly alkyl - water interactions.[61,62] It is clear from the inspection of density profiles that solubilities of alcohols in water are much smaller than solubilities of water in alcohols. Differences between solubilities increase as the molecular weight of the alcohol increases due to the presence of more unfavourable alkyl – water interactions in the system, as expected.

Density profiles of alcohols but also those of water exhibit an oscillatory behavior in the organic-rich liquid phase, near the interface between $z \approx -2$ and 0 nm. Particularly, the density profiles of alcohols show two clear relative maxima or peaks between the interface and the bulk region of the organic phase. This is especially true in the cases of hexan-1-

Table 6: Liquid density of the water-rich phase, $\rho^{(\mathbf{W})}$, liquid density of the organic-rich phase, $\rho^{(\mathbf{O})}$, molar fraction of water in the water-rich phase, $x_1^{(\mathbf{W})}$, molar fraction of water in the organic-rich phase, $x_1^{(\mathbf{O})}$, and interfacial tension, γ, of alcohol + water mixtures at 1 bar and different temperatures as obtained from MD $NP_z\mathcal{A}T$ simulations. The errors are estimated as explained in the text.

T (K)	$\rho^{(\mathrm{W})}$ (kg/m^3)	$\rho^{(\mathrm{O})}$ (kg/m^3)	$x_1^{(\mathrm{W})}$	$x_1^{(\mathrm{O})}$	γ (mN/m)
		butan-1-ol + water			
280	994(5)	848(4)	0.0117(5)	0.549(5)	3.0(4)
300	991(3)	824(5)	0.0099(4)	0.558(7)	3.1(5)
320	984(4)	803(4)	0.0084(6)	0.529(5)	3.3(4)
340	972(2)	798(4)	0.0093(2)	0.508(5)	3.6(4)
360	962(3)	775(4)	0.0093(5)	0.514(5)	3.1(3)
380	943(2)	761(4)	0.0098(4)	0.468(6)	2.6(2)
		pentan-1-ol + water			
280	996(1)	829(5)	0.0038(2)	0.67(1)	6.2(8)
300	996(2)	813(5)	0.0026(2)	0.67(1)	5.8(4)
320	991(1)	802(5)	0.0020(2)	0.648(9)	6.6(3)
340	980(1)	782(4)	0.0019(1)	0.626(6)	6.2(3)
360	969(1)	765(4)	0.0023(2)	0.585(8)	6.1(2)
380	950(1)	744(3)	0.0022(2)	0.571(4)	6.2(2)
		hexan-1-ol + water			
280	998(1)	829(4)	0.0010(1)	0.717(8)	7.8(9)
300	997(1)	813(4)	0.00053(9)	0.704(7)	7.5(7)
320	993(1)	800(4)	0.00052(5)	0.697(7)	9.1(4)
340	984(1)	783(4)	0.00038(5)	0.672(7)	9.6(3)
360	974(1)	770(4)	0.00051(6)	0.65(1)	8.5(4)
380	959(1)	743(5)	0.0009(1)	0.618(6)	8.0(3)
		heptan-1-ol + water			
280	998(1)	830(4)	0.00043(8)	0.74(1)	10.3(8)
300	998(2)	813(4)	0.00020(5)	0.75(1)	10.1(8)
320	994(1)	797(4)	0.00020(2)	0.75(1)	11.8(8)
340	986(1)	782(4)	0.00022(5)	0.71(1)	10.4(6)
360	976(1)	761(4)	0.00019(5)	0.701(9)	10.1(6)
380	962(1)	747(5)	0.00023(3)	0.617(9)	9.9(5)

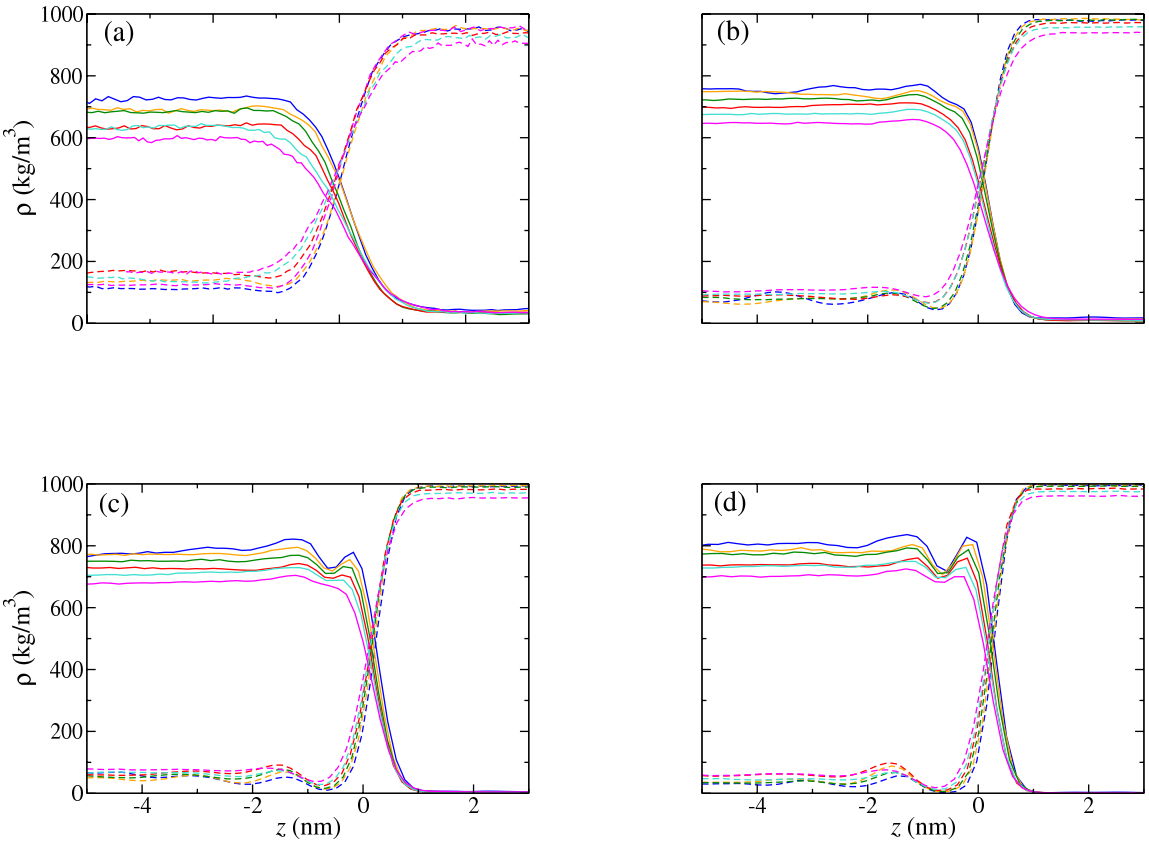

Figure 1: Simulated equilibrium density profiles $\rho(z)$ across the LL interface of alcohol (continuous curves) and water (dashed curves) as obtained from MD $NP_z\mathcal{A}T$ simulations of (a) butan-1-ol + water, (b) pentan-1-ol + water, (c) hexan-1-ol + water, and (d) heptan-1-ol + water mixtures at 1 bar and 280 (blue), 300 (orange), 320 (green), 340 (red), 360 (turquoise), and 380 K (magenta).

ol and heptan-1-ol. Although in the cases of butan-1-ol and pentan-1-ol is less clear, the analysis of the the behavior of molecular orientations presented below corroborates this issue. The oscillatory shape of the density profiles suggests a strong tendency of alcohol molecules to concentrate at the interface. A depression (desorption) of the profiles of alcohols and a complementary peak (adsorption) associated to profiles of water are also observed in the organic-rich phase, next to the interfacial region. These results indicate a self-organized structure of alcohol and water molecules near the interface. Although the real nature of the layer of alcohols and the accumulation of water molecules at the interface will be clear after the analysis of the molecular orientation of alcohol molecules (see discussion of Fig. 4 below), is obvious that structural ordering enhances as the molecular weight of the organic molecule increases. In other words, self-organization of the interface becomes more important as the number of alkyl groups (chain length) in alcohol molecules increases.

The behavior observed in the density profiles of alcohols and water molecules demonstrates partially the early hypothesis of Donahue and Bartell,[33] also followed by Ghatee and Ghazipour[28] and verified by Benjamin,[35] Jedlovszky *et al.*,[36] and Hantal *et al.*[37] In fact, although these authors proposed the formation of an oriented monolayer over the water surface, with the alcohol molecules adopting preferential orientation with the hydrophilic ends pointing towards the aqueous phase and the alkyl chains across the interface, our findings suggest the formation of a bilayer of alcohol molecules together with a small accumulation (adsorption) of water molecules in the organic-rich liquid phase. In particular, density profiles of Fig. 1 suggest the complete absence of water molecules in the space region between the two peaks observed in the density profiles of alcohols. In other words, there is a water-free region occupied mainly by the alkyl groups of the molecules forming the bilayer.

The hypothesis of the bilayer described in the previous paragraph is also corroborate looking at the interface with the "eyes" of MD. Fig. 2 shows snapshots extracted from MD trajectories of the simulation of butan-1-ol +, pentan-1-ol +, hexan-1-ol +, and heptan-1-ol + water mixtures. In the case of the butan-1-ol + water system, it is difficult to appreciate

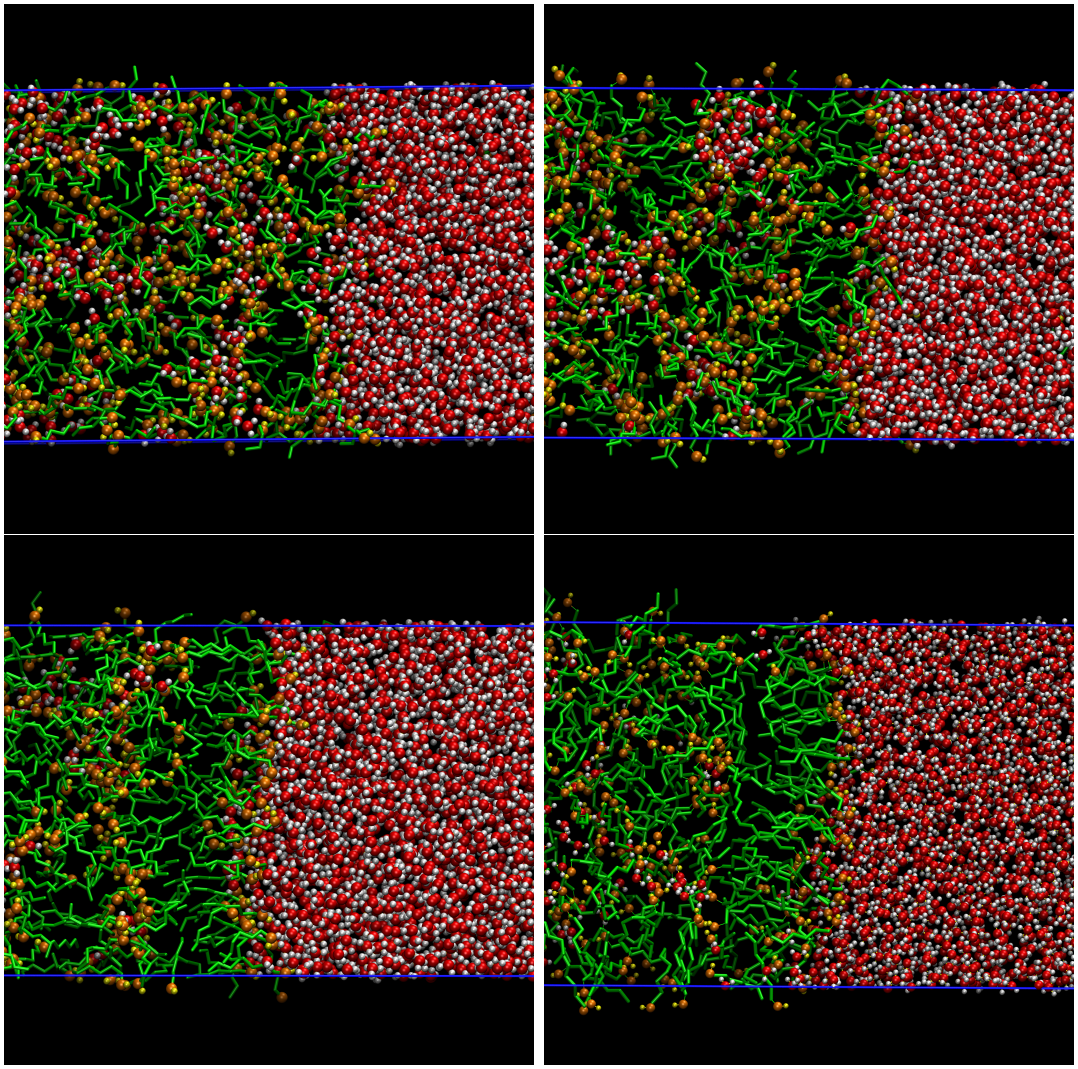

Figure 2: Snapshots of the LL interface obtained from MD $NP_z\mathcal{A}T$ simulations of the butan-1-ol + (top left), pentan-1-ol + (top right), hexan-1-ol + (bottom left), and heptan-1-ol + water (bottom right) mixtures at 1 bar and 280 K. Green licorice representation corresponds to alkyl groups of alcohols (CH_3 and CH_2 groups), orange and yellow spheres (van der Waals representation) to oxygen and hydrogen atoms in hydroxyl groups of alcohols, respectively, and red and white spheres to oxygen and hydrogen atoms in water molecules, respectively.

the existence of a stable bilayer or even a single layer of alcohol molecules near the interface. As the molecular weight of the alcohols increases, the formation of a first layer next to the aqueous phase, showing preferential orientation, is evident. Although snapshots only provide a static picture of these dynamic structures, movies obtained from MD simulations included in the Supporting Information provide additional evidences of the nature of the interface. Our main results presented in this paper concentrate on aqueous solutions of alcohols up to heptan-1-ol. However, as the self-organized structure of alcohols in contact with the water-rich phase enhances as the molecular weight of the alcohol is increased, we have also included additional graphical information of another system. In Fig. 3, we have depicted a snapshot extracted from the MD trajectory of the simulation of the octan-1-ol + water mixture. As it is apparent, there is a preferred orientational order of the alcohol molecules at the interface. A first layer is formed by alcohol molecules pointing its polar heads (OH groups) into the aqueous phase. This behavior has also been described by Benjamin,[35] Jedlovszky *et al.*,[36] and Hantal *et al.*[37] As it can be observed, the hydrophobic alkyl chain being rejected from the water-rich phase of the system results in a first layer of alcohol molecules oriented nearly parallel to z axis, i.e., perpendicular to the interface. A second layer of alcohol molecules is formed in such a way that polar heads (OH groups) point towards the organic-rich liquid phase, contrary to the first layer. Note that this second layer is located in a wider region of the space, according to Fig. 1, and it is seen less clearly in the snapshot. By inspecting the figure, it is easy to corroborate that the region between the two alcohol layers is water-free due to the alkyl – water unfavourable interactions. Although it is not clear to distinguish in the figure, a small adsorption of water molecules can be seen near the hydroxyl groups of alcohols in the second layer, in agreement with results shown in the density profiles of water (Fig. 1). Additional multimedia material is also included in the Supporting Information.

To gain physical insights into the structure of the interface, we analyze the molecular orientations of the alcohol molecules with respect to the interface. To this end, we define the end-to-end vector $\mathbf{d}$ that connects the centres of the two end carbon atoms of the alkyl chains

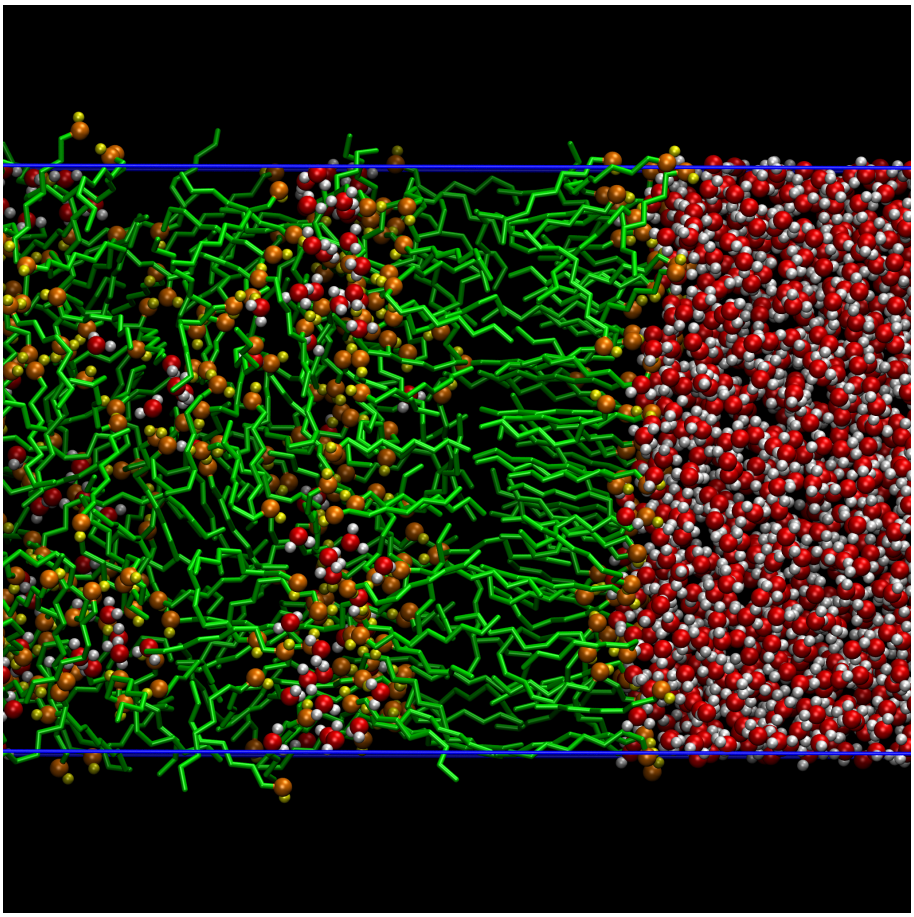

Figure 3: Snapshot of the LL interface obtained from a MD $NP_z\mathcal{A}T$ simulation of the octan-1-ol + water mixture at 1 bar and 280 K. Licorice and sphere representations are the same as in Fig. 2.

and that points towards the hydroxyl chemical group located at one end of the alcohol chain. This vector indicates the instantaneous direction of the alcohol chains and can be used to measure the possible orientation of the alcohol molecules with respect to the interface. Note that the modulus of $\mathbf{d}$ is the well-known end-to-end distance of the molecule. We also define the angle θ formed by the end-to-end vector with respect to the positive z-axis, the direction perpendicular to the interface, as

$$\mathbf{d} \cdot \hat{\mathbf{e}}_z = d \cos\theta \tag{5}$$

where $\hat{\mathbf{e}}_z$ is the unit vector along the z-axis and d is the distance between the centers of the two end atoms of the alcohol (end-to-end distance). With this definition, we compute for

each slab Δz along the z-direction of the simulation box the average angle formed by the end-to-end vector with respect to the z-axis, the direction perpendicular to the interface as

$$< \theta >= \left\langle \cos^{-1}\left(\frac{\mathbf{d}\cdot\hat{\mathbf{e}}_z}{d}\right)\right\rangle \tag{6}$$

The average values, $< \theta >$, are computed over all the alcohol molecules contained in each slab and cycle, and over the simulation production period. Obviously, the angle between the two defined vectors ranges between 0° and 180°. Note that when random orientation of the alcohol molecules exist in the slabs, averaged values of the angle θ should approach to 90°. This value is expected when no preferential orientation exits, i.e., far away from the LL interface, in the bulk homogeneous organic-rich and water-rich phases.

Fig. 4 shows the molecular orientations of alcohol molecules with respect to the interface. In particular, we depict the angle formed between the end-to-end vector and the z-axis, as a function of the position along the z-axis of the simulation box (perpendicular to the LL interface). As in the case of density profiles, the average orientation of the alcohol molecules along the interface normal is represented as a function of the center of mass of the molecule. As can be seen, the average angle of about 90º obtained far enough from the interface means a totally random orientation of the alcohol molecules in the bulk organic phase. Oppositely, the angle values obtained near the interface indicate a preferential orientation of the alcohol molecules, in consistency with the density profiles showed in Fig. 1 and the snapshots presented in Fig. 2 and also in Fig. 3. In particular, we find two main relative extrema or peaks at 40° and 110° that correspond to the two layers formed at $z \approx 0\,\text{nm}$ and $z \approx -1\,\text{nm}$, respectively. No peaks are found at 0° and 180°, angles that correspond to two layers of alcohols perfectly oriented perpendicular to the interface. This behavior is not expected due to fluctuations in the system (thermal agitation) and flexibility of alcohol chain molecules. It is worth noting that the fluctuating angle values in the aqueous phase are expected due to the small amount of alcohol molecules. In summary, the results presented in previous figures evidence the formation of a bilayer formed by alcohol molecules in the

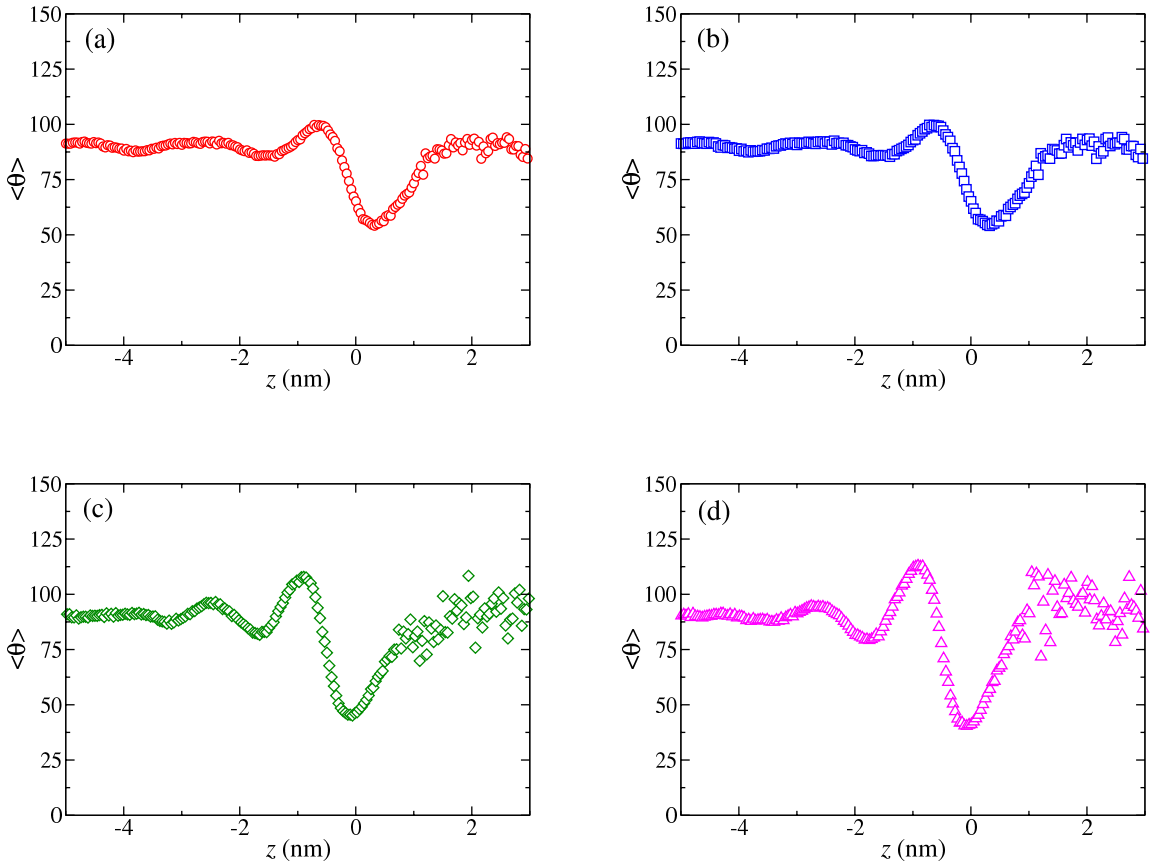

Figure 4: Equilibrium average angle, $< \theta >$, formed by the end-to-end vector with respect to the z-axis as obtained from MD $NP_z\mathcal{A}T$ simulations of (a) butan-1-ol + water (red circles), (b) pentan-1-ol + water (blue squares), (c) hexan-1-ol + water (green diamonds), and (d) heptan-1-ol + water (magenta triangles) mixtures at 1 bar and 280 K.

interface, with the first layer with hydroxyl groups pointing towards the aqueous phase at $z \approx 0\,\text{nm}$ and the second one with hydroxyl groups pointing to the opposite direction at $z \approx -1\,\text{nm}$. The longer the alcohol molecules are, the more stable the bilayer structure is.

It is also interesting to mention that the position of the maxima and minima corresponding to different alcohols slight vary as the chain length is varied: for butan-1-ol + water mixture, the position of the minimum is located at $z \approx -0.71\,\text{nm}$ and the maximum at $z \approx 0.32\,\text{nm}$, approximately, whereas for the case of the heptan-1-ol + water system, the position of the minimum is located at $z \approx -0.92\,\text{nm}$ and the maximum at $z \approx -0.07\,\text{nm}$, approximately.

The direct coexistence technique can be also used to compute solubilities, coexistence densities, and interfacial tension of mixtures. Coexistence densities in both liquid phases can be obtained from the analysis of the density profiles in regions at which liquids are homogeneous, i.e., the bulk regions of the simulation box. See the works of Algaba *et al.*[46,47] and Garrido *et al.*[63] for further details. Table 6 contains the compositions in both liquid phases as obtained from MD simulations. According to our goals, we now turn on the behavior of the temperature - composition or Tx projection of the phase diagrams of the alcohol + water systems. Fig. 5 shows the Tx projections at atmospheric pressure as obtained from MD simulations. In order to check the ability of the molecular models used in this work for predicting the equilibrium compositions of the mixtures, we have also included the corresponding experimental data taken from the literature.[42] As can be seen, the phase diagrams are dominated by large regions of LL immiscibility. This is a consequence of the interplay between different effects: (1) favourable water – water and water – alcohol hydrogen bonding interactions; (2) unfavourable alkyl – water interactions; (3) compositional and orientational entropic effects through hydrogen bonding; and (4) excluded volume effects due to elongation and flexibility of alcohols. Unfavourable interactions become more important as the molecular weight of the alcohol increases since the number of water – alkyl group interactions is larger. This effect leads to an enlargement of the closed-loop of immiscibility

as the alcohols become longer, decreasing the mutual solubilities of both components.

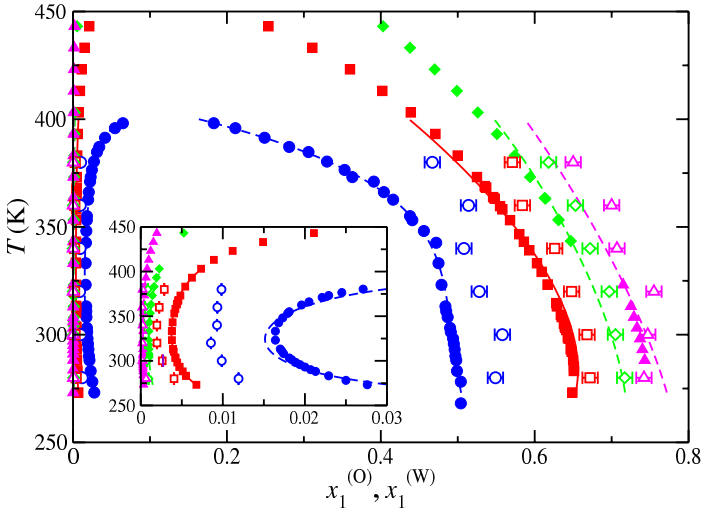

Figure 5: Tx projection of the phase diagram of the butan-1-ol + (blue symbols), pentan-1-ol + (red symbols), (c) hexan-1-ol + (green symbols), and heptan-1-ol + water (magenta symbols) mixtures at 1 bar. Filled symbols correspond to experimental data taken from the literature,[42] open symbols to MD $NP_z\mathcal{A}T$ simulations obtained in this work, and dashed curves to correlations from literature.[42] $x_1^{(O)}$ and $x_1^{(W)}$ are the molar fractions of alcohols in the organic-rich and aqueous-rich phases, respectively.

For a given member of the alcohol homologous series, immiscibility decreases as the temperature is increased. This is an expected result since the contribution to the free energy associated to compositional and orientational entropy becomes larger as the temperature is raised. Note that thermal agitation makes less stable the water – alcohol hydrogen bonds, resulting in an increase of both entropic contributions. As temperature is further increased, the phase envelop of the butan-1-ol + water mixture closes at an UCST at 400 K approximately. It seems that the rest of mixtures (from pentan-1-ol up to heptan-1-ol aqueous solutions) should behave in a similar way, although unfortunately no experimental information is available.

According to experimental data[10,11] and predictions from molecular-based approaches,[12,13] the mixture exhibits type VI phase behavior. This means that mutual solubilities of water and butan-1-ol decrease as temperature is raised. This behavior is seen in Fig. 5, not only for

experiments but also for predictions obtained from computer simulations (see the inset of the figure in which the curvature of the phase envelope corresponding to the aqueous-rich phase indicates that solubilities of alcohols in water decrease as temperature is increased). The shape of the phase envelopes are clearly related with the closing of the LL immiscibility loop at low temperatures. Unfortunately, at these conditions the LCST of the butan-1-ol + water mixture is not present since is located inside the solid boundaries of the system, and the situation is even worse for longer alcohols for which solid phases are stable at higher temperatures.[10–13] Our findings, using well-established molecular-based models and computer simulation techniques, agree with experimental data taken from the literature[42] and confirm the original hypothesis of Donahue and Bartell,[33] also followed by Villers and Platten[26] and Tian *et al.*,[27] i.e., solubilities of alcohols in water exhibit a minima with temperature. According to the literature, this behavior must be related with the unusual dependence of the interfacial tension with temperature. We check now that molecular models used in this work are able to capture this phenomenon.

We also present here additional results obtained from MD simulations of the LL interface of aqueous solutions of alcohols. In particular, we focus on the effect of temperature and molecular weight of the organic component on coexistence densities. Liquid coexistence densities can be obtained following the same approach used for compositions, i.e., from the analysis of the density profiles along the corresponding bulk regions of both liquids.[46,47,63] Coexistence density values obtained in this work from MD simulations are presented in Table 6.

Temperature - density or $T\rho$ projections of the phase diagram of aqueous solutions of linear alcohols are depicted in Fig. 6. Liquid densities decrease as the temperature of the system is increased. The decrease is more pronounced in the case of the organic phase since density of the aqueous phase is nearly constant in a wide range of temperatures. Predictions obtained from molecular simulations are able to capture this general behavior of the system. This effect is related obviously with an enhancement of the molecular thermal agitation of

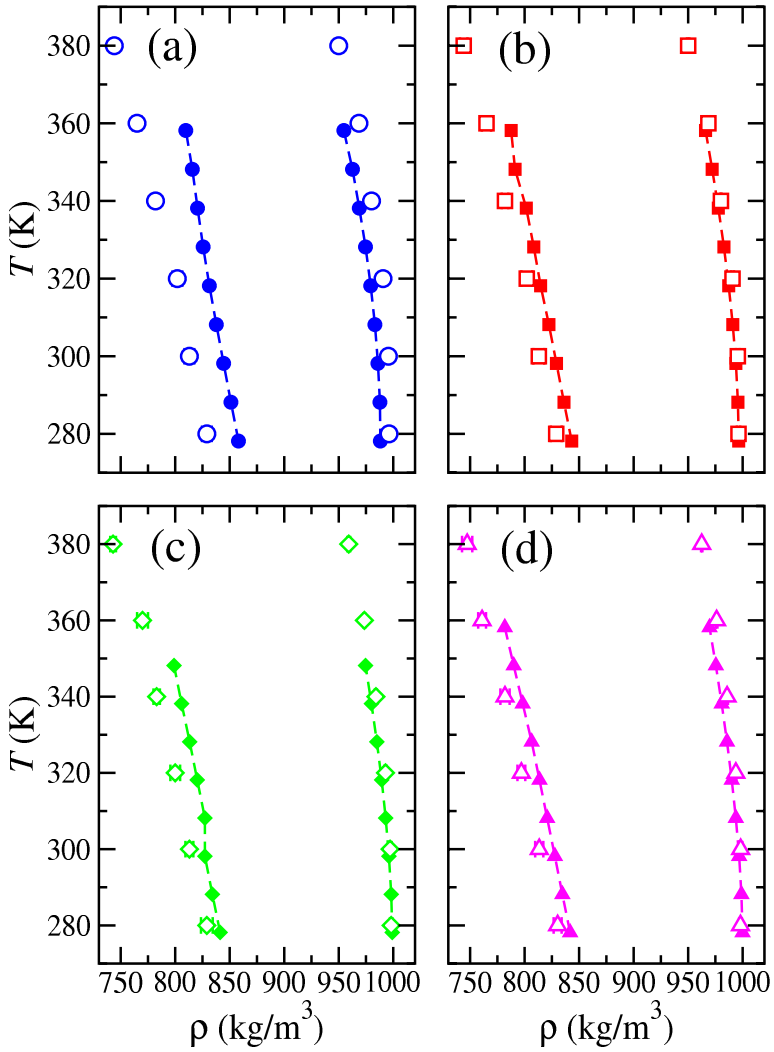

Figure 6: $T\rho$ projection of the phase diagram of the (a) butan-1-ol + (blue circles), (b) pentan-1-ol + (red squares), (c) hexan-1-ol + (green diamonds), and (d) heptan-1-ol + water (magenta triangles) mixtures at 1 bar. Filled symbols and curves correspond to experimental data taken from the literature[29] and open symbols to MD $NP_z\mathcal{A}T$ simulation results obtained in this work.

the system that induces a volume increment in both phases, with the corresponding decrease of density as the temperature is raised. It is also interesting to analyze the effect of increasing the molecular weight of alcohols that is less evident than in the case of temperature. Now, the major effect, when passing from the butan-1-ol + water mixture to the pentan-1-ol + water system, is the decrease of the density of the organic-rich phase and the increase the density of the aqueous phase. Note that the change of density is larger in the case of the alcohol-rich liquid phase density. A further increase of the molecular weight of the alcohol (passing from pentan-1-ol to hexan-1-ol and heptan-1-ol) leaves the $T\rho$ slides of the phase diagram nearly identical. It is interesting to check that predictions from simulations are able to capture this effect in all cases.

This behavior can be explained qualitatively in terms of unlike intermolecular interactions, solubilities of alcohols in water, and excluded volume effects. In the case of the water-rich liquid phase, the increasing of the liquid density can be explained in terms of the unlike interactions between the alkyl chemical groups and water molecules. When passing from butan-1-ol to pentan-1-ol, the mean number of alkyl groups in the phase increases. Due to the alkyl-water unfavourable interactions, the solubility of the alcohol in water decreases (see Fig. 5 of the main article). In average, the number of pentan-1-ol molecules in the water-rich phase decreases in comparison with those of butan-1-ol. Consequently, water molecules can accommodate better in the available space in the phase, increasing the number of effective water hydrogen bonds (favourable interactions), and increasing effectively the liquid density. In the case of the organic-rich liquid phase, the situation is slightly different. Now, an increase of the length of the alcohol molecules (when passing from butan-1-ol to pentan-1-ol) produces an increase of the excluded volume. Note that, due to packing effects, the number of organic molecules is much larger than the number of water molecules, and there is a small energetic penalty in the system due to the alkyl-water unfavourable intermolecular interactions. As a consequence of that, an increase of the average volume of the system exists, and effectively, the density of the organic-rich liquid phase decreases. These

effects, that occur for different reasons in both phases and produce small changes in the phase diagram of the systems under study, become negligible in the cases of hexan-1-ol and heptan-1-ol, observing finally a limiting behavior in both predictions and experiments.

Agreement between simulation results and experimental data taken from the literature is in general good, especially for the density values of the aqueous phase. The density of the organic phase is underestimated in all cases, especially for the butan-1-ol + water binary system. As the molecular weight of the alcohol increases, differences between the predicted and experimental organic density values decrease. The same is true for the density of the aqueous phase although in this case the agreement between both results is really quantitative. TIP4P/2005 is probably the best rigid and nonpolarizable water model in the literature.[38] In particular, it is able to predict a great number of thermodynamic properties, including vapor-liquid (and solid) coexistence, vapor pressure, enthalpies of vaporization, surface tension, etc.[39,64,65] The same can be said about the molecular models for alcohols. The TraPPE models are well established force fields that are able to provide very accurately different thermodynamic properties, such as vapor-liquid coexistence and vapor pressure.[41] In general, one can say that these models are able to predict quantitatively the phase behavior of pure water and alcohol systems. Then, why predictions from simulation are not quantitative, especially in the case of the butan-1-ol + water binary mixture? Why differences between simulation predictions and experimental data are larger in the organic-rich phase than in the water-rich phase? Why differences seem to decrease as the molecular weight of the alcohol is higher? And finally, why agreement between both results is better at low temperatures and seems to be worse at high temperatures?

We think differences between simulation and experiments in both phases, but especially in the case of the organic phase, could be answered using a combination of three arguments: (1) the incompatibility of two sets of models, pure water and the homologous series of alcohols; (2) the effect of temperature; and (3) the mutual solubilities of alcohols and water.

In general, discrepancies between simulation results and experimental data in both liquid

phases are mainly observed when compositions of both components are comparable, or in other words, when both components are significantly present in a phase, i.e., the organic-rich liquid phase. We think the failure of the mixture model in predicting the properties of the mixtures comes from the fact that, although the models for water and alcohol work very well for pure systems, they were developed independently from each other, and have not been optimized together. Obviously, the lost of accuracy in predicting mixture properties is less pronounced in the case of the water-rich liquid phase. This phase can be considered nearly a pure water phase since composition of alcohols is negligible in most cases (except for the butan-1-ol + water mixture). The incompatibility of water and alcohol models is even worse if we take into account that the alcohol + water systems that exhibit large regions of LL immiscibility in the phase diagram. The high non-ideality of these systems is a consequence of a delicate interplay between the water-water and water-alcohol hydrogen bonding interactions, the unfavourable interactions between the alkyl chemical groups and water molecules, and excluded volume effects associated with the chain-like character of alcohol molecules. These effects could explain qualitatively why the molecular models used in this work, the TIP4P/2005 and TraPPE force fields, are unable to account for correctly the experimental liquid densities, especially for low molecular weight alcohols and in the organic-rich liquid phase.

However, the incompatibility of the two models alone can not explain why differences between simulation and experiments are higher in the organic phase than in the aqueous phase. It is also necessary to include one of the key ingredients in this discussion: the mutual solubilities of alcohols and water. As it is shown in Fig. 4 of the main article, the solubility of water in the organic-rich phase is much higher than that of alcohols in water. This effect is related with the hydrogen bonding interactions between water molecules, the unlike alkyl-water interactions, and the difference in size between the components of the system. In the case of the butan-1-ol + water binary mixture, the effective number of alcohol-water interactions in the aqueous phase is smaller than in the organic phase. The incompatibility

of the models produces errors in predictions when both components are present in the phase, or in other words, when the number of effective interactions between both components increases. This argument also allows to explain why the agreement between simulation and experiment improves as the molecular weight of alcohols increases: heavier alcohols contain more alkyl groups, decreasing the mutual solubility between both components. Since the effective number of alcohol-water interactions also decrease, the contribution to the intermolecular energy due to the unlike interactions is also lower, and agreement between simulation and experiment improves. Obviously, this effect could be corrected if molecular parameters of water and alcohol models are optimized together.

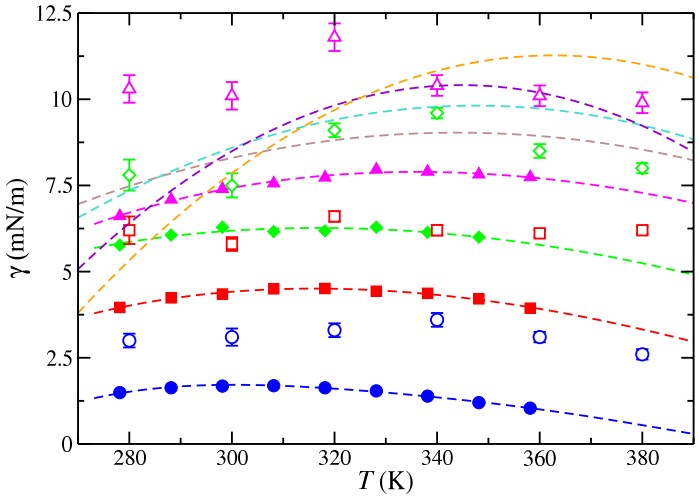

Figure 7: LL interfacial tension as a function of temperature of the butan-1-ol + (blue symbols), pentan-1-ol + (red symbols), hexan-1-ol + (green symbols), heptan-1-ol + water (magenta symbols), octan-1-ol + water (brown curve), nonan-1-ol + water (turquoise curve), decan-1-ol + water (violet curve), and dodecan-1-ol + water (orange curve) mixtures at 1 bar. Filled symbols correspond to experimental data taken from the literature,[29] open symbols to MD $NP_z\mathcal{A}T$ simulations obtained in this work, and dashed curves to the fitting of the experimental interfacial tension values to parabolic curves.

Temperature also affects agreement between predictions obtained from computer simulation and experimental data. This is easily explained since mutual solubilities depend on temperature. As the temperature increases, solubilities increase (especially in the case of the organic-rich phase) as the compositional and orientational entropic contributions to the

free energy overcome the unfavourable energetic contributions. According to our previous discussion, an increase of the mutual solubility provokes more alcohol-water interactions, a situation in which the incompatibility of both models increases, which results in a poorer agreement between simulation and experiments. This effect is more noticeable for the organic phase, as it was explained previously.

Finally, we consider in Fig. 7 the LL interfacial tension of the alcohol + water mixtures from MD simulations. In addition to that, we have also represented the experimental data taken from the literature[29] in order to check the ability of the molecular models for predicting this sensitive interfacial property. As can be seen in the figure, the interfacial tension of the butan-1-ol + water mixture shows a parabolic behavior with the temperature. In particular, the interfacial tension at low temperatures increases with the temperature and reaches a relative maximum value. However, at high temperatures, the interfacial tension decreases as the temperature is further increased.

The same behavior is observed for the interfacial tension curves of mixtures with heavier alcohols. However, two important differences can be seen in curves as the chain length of the alcohol is increased. Firstly, the range of interfacial tension values increases as the alcohol is heavier. In particular, the relative maximum value reached by the interfacial tension increases with increasing the molecular weight of the alcohol. These effects are expected since interfacial tension increases as the phase separation is larger.[29,42] Secondly, the temperature at which the maximum value of the interfacial tension is reached increases nearly linearly with the molecular weight of alcohols.

The TIP4P/2005 and TraPPE molecular models are able to capture the main features of the behavior exhibited by the LL interfacial tension of the alcohol + water mixtures: the parabolic behavior with temperature, the existence of a relative maximum value for the interfacial tension, larger values of the interfacial tension as the molecular weight of alcohols is increased, and an increase of the temperature at which the maximum of the interfacial tension value is reached. Despite the overall qualitative agreement between computational

and experimental results in predicting interfacial tension for our systems, quantitative differences are evident. The computed values are overestimated in about 10-30 % percent. In this sense, it is worthwhile remarking that to accurately predict LL interfacial tension is computationally challenging. It is a property extremely sensitive to the molecular details and to other simulation details, such as the cutoff radius, box size, and number of particles, among others.[52,66–70] Besides, it is important to recall that the molecular parameters of the models used in this work have been independently optimized to predict the phase behavior of pure fluids and not the mixture properties. Although the mixture model exhibits limitations for quantitatively predicting the experimental data taken from the literature, we think it is able to provide, in general, a good simultaneous predictions for the phase equilibria, including $T\rho$ and Tx projections of the phase diagram, as well as for the LL interfacial tension of complex aqueous solutions of alcohols.

Conclusion

We have analyzed, from a microscopic perspective, LL interfaces of aqueous solutions of alcohols, with particular emphasis on the structure and formation of layers of the organic compounds oriented preferentially at the alcohol-water interfaces. In addition to that, and taking advantage of the same microscopic models, we have provided physical insights into the unusual behavior of the interfacial tension between long-chain alcohols and water, and its connection with the apparent anomalous mutual solubilities at low temperatures from a molecular level. Predictions are obtained combining $NP_z\mathcal{A}T$ or isothermal-isobaric MD simulations, the direct simulation technique, and simple but accurate molecular models for water (TIP4P/2005) and linear alcohols (TraPPE-UA) that explicitly account for the most salient microscopic features of aqueous solutions of alcohols. In this contribution, we have considered aqueous mixtures of alcohols from the butan-1-ol + up to the octan-1-ol + water system.

Simulation results for density profiles of water and alcohols and a careful analysis of the relative orientation of the alcohol molecules near the LL interfaces indicate that aqueous solutions of alcohols show a self-organized structure of the organic compounds in contact with the water-rich liquid phase that is enhanced as the molecular weight of the alcohol increases. In particular: (a) a first layer is formed by alcohol molecules pointing its polar heads (OH groups) into the aqueous phase; (b) the hydrophobic alkyl chains are rejected from the water-rich phase, provoking an orientation of the molecules nearly perpendicular to the interface; (c) a second layer of alcohol molecules is formed in such a way that polar heads (OH) point towards the organic-rich liquid phase; (d) the region between the two alcohol layers is water-free; and (e) a small adsorption of water molecules is formed near the hydroxyl groups of alcohols in the second layer. Results, also corroborated by snapshots and movies obtained from microscopic trajectories, provide a precise picture of the interfacial behavior suggested by previous authors in the literature.[28,33]

We have also analyzed carefully the thermodynamic behavior of the systems, particularly the temperature-density and temperature-composition projections of the phase diagrams. The molecular models predict a decrease of mutual solubilities of both compounds at low temperatures, in agreement with experiments and the hypothesis proposed by Donahue and Bartell,[33] Villers and Platten,[26] and Tian *et al.*,[27] i.e., solubilities of alcohols in water exhibit a minima with temperature. According to the literature and our findings, this behavior must be related with the unusual dependence of the interfacial tension with temperature.

TIP4P/2005 and TraPPE models are able to capture the main features of the behavior shown by the LL interfacial tension of aqueous solutions of alcohols originally discovered by Villers and Platten:[26] (a) parabolic behavior with temperature; (b) existence of a relative maximum value of interfacial tension; (c) larger values of interfacial tension as the molecular weight of alcohols is increased; and (d) increase of the temperature at which the maximum is reached as alcohols are longer.

Finally, agreement between simulation predictions and experimental data taken from the

literature is good, including coexistence densities, liquid compositions, and also interfacial tension values. This is especially true taking into account that simulation results are predictions obtained from molecular parameter values optimized independently to provide an accurate description of the phase equilibria of alcohols and water. This means that mixture properties are obtained using the well-known Lorentz-Berthelot combining rules. This approach, which is probably the most direct and simplest way to describe mixtures from pure components, is not particularly appropriate for highly non-ideal systems, such as aqueous solutions of alcohols. These mixtures are dominated by large regions of immiscibility controlled by a delicate interplay between hydrogen bonding specific interactions (alcohol-alcohol, water-water, and alcohol-water). Clearly, it would be possible to parameterize the models to make them working well also for mixtures. However, it is encouraging to check that this simple approach is able to provide the correct picture of the macroscopic and microscopic behavior of these complex mixtures from a truly molecular perspective.

Acknowledgement

We acknowledge Centro de Supercomputación de Galicia (CESGA, Santiago de Compostela, Spain) and MCIA (Mésocentre de Calcul Intensif Aquitain) of the Universités de Bordeaux and Pau et Pays de l'Adour (France), for providing access to computing facilities and Ministerio de Economía, Industria y Competitividad through Grant with reference FIS2017-89361-C3-1-P co-financed by EU FEDER funds. Further financial support from Junta de Andalucía and Universidad de Huelva is also acknowledged. J.A.F. acknowledges Contrato Predoctoral de Investigación from XIX Plan Propio de Investigación de la Universidad de Huelva and a FPU Grant (Ref. FPU15/03754) from Ministerio de Educación, Cultura y Deporte. J. A., J. M. M., P. G.-A., and F. J. B. thankfully acknowledge the computer resources at Magerit and the technical support provided by the Spanish Supercomputing Network (RES) (Project QCM-2018-2-0042). A.M. and M.C. also acknowledges the financial support of FONDECYT,

Chile (Project 1190107).

References

(1) Rowlinson, J. S.; Swinton, F. L. *Liquids and Liquid Mixtures*; Butterworth, London, 1982.

(2) Gorak, A.; Olujic, Z. *Distillations: Equioment and Processes*; Academic Press, 2014.

(3) Bart, H.-J. *Reactive Extraction*; Springer, Berlin, Heidelberg, 2001.

(4) Davies, J. T.; Rideal, E. K. *Interfacial Phenomena*; Academic Press, New York, 1961.

(5) Bresme, F.; Chacón, E.; Tarazona, P. Molecular dynamics investigation of the intrinsic structure of water–fluid interfaces via the intrinsic sampling method. *Phys. Chem. Chem. Phys.* **2008**, *10*, 4704–4715.

(6) Danesh, A. *PVT and Phase Behaviour of Petroleum Reservoir Fluids*; Elsevier, Amsterdam, 2007.

(7) Pedersen, K. S.; Christensen, P. L. *Phase Behaviour of Petroleum Reservoir Fluids*; CRC Press, Boca Raton, 2007.

(8) Dandekar, A. *Petroleum Reservoir Rock and Fluid Properties*; CRC Press, Boca Raton, 2007.

(9) Landmeyer, J. E.; Bradley, P. M.; Trego, D. A.; Hale, K. G.; Haas, J. E. MTBE, TBA, and TAME Attenuation in Diverse Hyporheic Zones. *Ground Water* **2010**, *48*, 30–41.

(10) Schneider, G. M. High-Pressure Investigations on Fluid System - A Challenge to Experiment, Theory and Application. *Pure Applied Chemistry* **1991**, *63*, 1313–1326.

(11) Ochel, H.; Becker, H.; Maag, K.; Schneider, G. M. Influence of a Third Component on (Liquid + Liquid) Phase Equilibria in (Butan-2-ol + Water) and in (Butan-1-ol + Water) at Pressures up to 160 MPa. *J. Chem. Thermodynamics* **1993**, *25*, 667–677.

(12) García-Lisbona, M. N.; G., A.; Jackson, G.; Burgess, A. N. Predicting the High-Pressure Phase Equilibria of Binary Aqueous Solutions of 1-Butanol, n-Butoxyethanol and n-Decylpentaoxyethylene Ether ($C_{10}E_5$)Using the SAFT-HS Approach. *Mol. Phys.* **1998**, *93*, 57–71.

(13) García-Lisbona, M. N.; G., A.; Jackson, G.; Burgess, A. N. An Examination of the Cloud Curves of Liquid-Liquid Immiscibility in Aqueous Solutions of Alkyl Polyoxyethylene Surfactants Using the SAFT-HS Approach with Transferable Parameters. *J. Am. Chem. Soc.* **1998**, *120*, 4191–4199.

(14) Scott, R. L.; Konynenburg, P. H. V. Static Properties of Solutions. Van Der Waals and Related Models for Hydrocarbon Mixtures. *Discuss. Faraday Soc.* **1970**, *49*, 87–97.

(15) Konynenburg, P. H. V.; Scott, R. L. Critical Lines and Phase Equilibria in Binary Van Der Waals Mixtures. *Phil. Trans.* **1980**, *A298*, 495–540.

(16) Deiters, U. K.; Kraska, T. *High-pressure Fluid Phase Equilibria (Phenomenology and Computation)*; Elsevier, Amsterdam, 2012.

(17) Hirschfelder, J.; Stevenson, D.; Eyring, H. A Theory of Liquid Structure. *J. Chem. Phys.* **1937**, *5*, 896–912.

(18) Hudson, C. S. Die Gegenseitige Löslichkeit von Nikotin in Wasser. *Z. Phys. Chem.* **1904**, *47*, 113–114.

(19) Dolgolenko, W. Nonionic Surfactant Mixtures. I. Phase Equilibria in $C_{10}E_4$–H_2O and Closed-Loop Coexistence. *Z. Phys. Chem.* **1908**, *62*, 499.

(20) McEwan, B. C. CCLVI.—Studies in Mutual Solubility. Part II. The Mutual Solubility of Glycerol and Alcohols, Aldehydes, Phenols, and Their Derivatives. *J. Chem. Soc. Trans.* **1923**, *123*, 2284–2288.

(21) Andon, R. J. L.; Cox, J. D. 896. Phase Relationships in the Pyridine Series. Part I. The Miscibility of Some Pyridine Homologues with Water. *J. Chem. Soc.* **1952**, *1952*, 4601–4606.

(22) Lang, J. C.; Morgan, D. R. Nonionic Surfactant Mixtures. I. Phase Equilibria in $C_{10}E_4$–H_2O and Closed-Loop Coexistence. *J. Chem. Phys.* **1980**, *73*, 5849–5861.

(23) Mittal, K. L.; Lindman, B. *Surfactants in Solutions, Vols. 1-3*; Plenum, 1984.

(24) Nord, F. F.; Bier, M.; Timasheeff, S. N. Investigations on Proteins and Polymers. IV.1 Critical Phenomena in Polyvinyl Alcohol-Acetate Copolymer Solutions. *J. Am. Chem. Soc.* **1951**, *73*, 289–293.

(25) Malcolm, G. N.; Rowlinson, J. S. The Thermodynamics Properties of Aqueous Solutions of Polyethylene Glycol, Polypropylene Glycol and Dioxane. *Trans. Faraday Soc.* **1957**, *53*, 921–931.

(26) Villers, D.; Platten, J. K. Temperature Dependence of the Interfacial Tension Between Water and Long-Chain Alcohols. *J. Phys. Chem.* **1988**, *92*, 4023–4024.

(27) Tian, Y.; Cao, L.; Qiu, L.; Zhu, R. Comparison Study on Temperature Dependence of the Interfacial Tension of n-Alkane-Water and n-Alcohol-Water Two Binary Systems. *J. Chem. Eng. Data* **2014**, *59*, 3495–3501.

(28) Ghatee, M. H.; Ghazipour, H. Highly Accurate Liquid-Liquid Interfacial Tension Measurement by a Convenient Capillary Apparatus. *Fluid Phase Equil.* **2014**, *377*, 76–81.

(29) Cárdenas, H.; Cartes, M.; Mejía, A. Atmospheric Densities and Interfacial Tensions for

1-Alkanol (1-Butanol to 1-Octanol)+ Water and Ether (MTBE, ETBE, DIPE, TAME and THP)+ Water Demixed Mixtures. *Fluid Phase Equil.* **2015**, *396*, 88–97.

(30) del Pozo, I.; Cartes, M.; Llovell, F.; Mejía, A. Densities and Interfacial Tensions for Fatty Acid Methyl Esters (from Methyl Formate to Methyl Heptanoate) + Water Demixed Mixtures at Atmospheric Pressure Conditions. *J. Chem. Thermodynamics* **2018**, *121*, 121–128.

(31) Domańska, U.; Królikowska, M. Effect of Temperature and Composition on the Surface Tension and Ahermodynamic Properties of Binary Mixtures of 1-Butyl-3-Methylimidazolium Thiocyanate with Alcohols. *J. Colloid Interf. Sci.* **2010**, *348*, 661–667.

(32) Reyes, G.; Cartes, M.; ands H. Segura, C. R.-C.; Mejía, A. Surface tension of 1-ethyl-3-methylimidazolium ethyl sulfate or 1-butyl-3-methylimidazolium hexafluorophosphate with argon and carbon dioxide. *J. Chem. Eng. Data* **2013**, *58*, 1203–1211.

(33) Donahue, D. J.; Bartell, F. E. The Boundary Tension at Water-Organic Liquid Interfaces. *J. Phys. Chem.* **1953**, *56*, 480–484.

(34) Ssementschenko, V. W.; Gratschewa, S.; Davidoffskaja, E. Gegenseitige Löslichkeit und Oberflächenspannung. *Kolloid. Z.* **1934**, *68*, 275–286.

(35) Benjamin, I. Polarity of the water/octanol interface. *Chem. Phys. Lett.* **2004**, *393*, 453–456.

(36) Jedlovszky, P.; Varga, I.; Gilányi, T. Adsorption of 1-octanol at the free water surface as studied by Monte Carlo simulation. *J. Chem. Phys.* **2004**, *120*, 11839–11851.

(37) Hantal, G.; Fábian, B.; Sega, M.; Jedlovszky, P. Contribution of the two liquid phases to the interfacial tension at various water-organic liquid-liquid interfaces. *J. Mol. Liq.* **2020**, *306*, 112872–1–112872–10.

(38) Abascal, J. L.; Vega, C. A General Purpose Model for the Condensed Phases of Water: TIP4P/2005. *J. Chem. Phys.* **2005**, *123*, 234505/1–12.

(39) Vega, C.; Miguel, E. D. Surface Tension of the Most Popular Models of Water by Using the Test-Area Simulation Method. *J. Chem. Phys.* **2007**, *126*, 154707.

(40) Míguez, J. M.; González-Salgado, D.; Legido, J. L.; Piñeiro, M. M. Calculation of Interfacial Properties Using Molecular Simulation with the Reaction Field Method: Results for Different Water Models. *J. Chem. Phys.* **2010**, *132*, 184102.

(41) Chen, B.; Potoff, J. J.; Siepmann, J. I. Monte Carlo Calculations for Alcohols and Their Mixtures with Alkanes. Transferable Potentials for Phase Equilibria. 5. United-Atom Description of Primary, Secondary, and Tertiary Alcohols. *J. Phys. Chem. B* **2001**, *105*, 3093–3104.

(42) Góral, M.; B-Wiśniewska-Goclowska,; A, M. Recommended Liquid-Liquid Equilibrium Data. Part 4. 1-Alkanol-Water Systems. *J. Chem. Ref. Data* **2006**, *35*, 1391–1414.

(43) Mejía, A.; Cartes, M.; Segura, H.; Müller, E. A. Use of Equations of State and Coarse Grained Simulations to Complement Experiments: Describing the Interfacial Properties of Carbon Dioxide+ Decane and Carbon Dioxide+ Eicosane Mixtures. *J. Chem. Eng. Data* **2014**, *50*, 2928–2941.

(44) Müller, E. A.; Jackson, G. Force Field Parameters from the SAFT-γ Equation of State for Use in Coarse-Grained Molecular Simulations. *Annu. Rev. Chem. Biomol. Eng.* **2014**, *5*, 405–427.

(45) Míguez, J. M.; Garrido, J. M.; Blas, F. J.; Segura, H.; Mejía, A.; Piñeiro, M. M. Comprehensive Characterization of Interfacial Behavior for the Mixture $CO_2 + H_2O + CH_4$: Comparison Between Atomistic and Coarse Grained Molecular Simulation Models and Density Gradient Theory. *J. Phys. Chem. C* **2014**, *118*, 24504–24519.

(46) Algaba, J.; Garrido, J. M.; Míguez, J. M.; Mejía, A.; Bravo, A. I. M.-V.; Blas, F. J. Interfacial Properties of Tetrahydrofurane and Carbon Dioxide Mixture from Computer Simulation. *J. Phys. Chem. C* **2018**, *122*, 16142–16153.

(47) Algaba, J.; Cartes, M.; Mejía, A.; Míguez, J. M.; Blas, F. J. Phase Equilibria and Interfacial Properties of the Tetrahydrofuran + Methane Binary Mixture from Experiment and Computer Simulation. *J. Phys. Chem. C* **2019**, *123*, 20960–20970.

(48) Feria, E.; Algaba, J.; Míguez, J. M.; Mejía, A.; Gómez-Álvarez, P.; Blas, F. J. Vapour-Liquid Phase Equilibria and Interfacial Properties of Fatty Acid Methyl Esters from Molecular Dynamics Simulations. *Phys. Chem. Chem. Phys.* **2020**, *22*, 4974–4983.

(49) van der Spoel, D.; Lindahl, E.; Hess, B.; Groenhof, G.; Mark, A. E.; Berendsen, H. J. GROMACS: Fast, Flexible, and Free. *J. Comput. Chem.* **2005**, *26*, 1701–1718.

(50) Galliero, G.; Piñeiro, M. M.; Mendiboure, B.; Miqueu, C.; Lafitte, T.; Bessieres, D. Interfacial Properties of the Mie n-6 Fluid: Molecular Simulations and Gradient Theory Results. *J. Chem. Phys.* **2009**, *130*, 104704/1–10.

(51) Galliero, G. Surface Tension of Short Flexible Lennard-Jones Chains: Corresponding States Behavior. *J. Chem. Phys.* **2010**, *133*, 074705/1–7.

(52) Míguez, J. M.; Piñeiro, M. M.; Blas, F. J. Influence of the Long-Range Corrections On the Interfacial Properties of Molecular Models Using Monte Carlo Simulation. *J. Chem. Phys.* **2013**, *138*, 034707/1–11.

(53) Cuendet, M. A.; Gunsteren, W. F. V. On the Calculation of Velocity-Dependent Properties in Molecular Dynamics Simulations Using the Leapfrog Integration Algorithm. *J. Chem. Phys.* **2007**, *127*, 184102/1–9.

(54) Nosé, S. A Molecular Dynamics Method for Simulations in the Canonical Ensemble. *Mol. Phys.* **1984**, *52*, 255–268.

(55) Parrinello, M.; Rahman, A. *J. Appl. Phys.* **1981**, *52*, 7182.

(56) Berendsen, H. J. C.; Postma, J. P. M.; Gunsteren, W. F. V.; Nola, A. D.; Haak, J. R. Molecular Dynamics with Coupling to an External Bath. *J. Chem. Phys.* **1984**, *81*, 3684/1–8.

(57) Hulshof, H. Ueber Die Oberflachenspannung. *Ann. Phys. (Berlin)* **1901**, *4*, 165–186.

(58) Rowlinson, J. S.; Widom, B. *Molecular Theory of Capillarity*; Claredon Press, 1982.

(59) Miguel, E. D.; Blas, F. J.; Río, E. M. D. Molecular Simulation of Model Liquid Crystals in a Strong Aligning Field. *Mol. Phys.* **2006**, *104*, 2919–2927.

(60) Miguel, E. D.; Jackson, G. The Nature of the Calculation of the Pressure in Molecular Simulations of Continuous Models from Volume Perturbations. *J. Chem. Phys.* **2006**, *125*, 164109/1–12.

(61) Vochten, R.; Petre, G. Study of the Heat of Reversible Adsorpotion at The Air-Solution Interface. II. Experimental determination of the Heat of Reservible Adsorption of Some Alcohols. *J. Colloid Interf. Sci.* **1973**, *42*, 320–327.

(62) Shinoda, K. "Iceberg" Formation and Solubility. *J. Phys. Chem.* **1977**, *81*, 1300–1302.

(63) Garrido, J. M.; Quinteros-Lama, H.; J, M. M.; Blas, F. J.; Piñeiro, M. M. On the Physical Insight into the Barotropic Effect in the Interfacial Behavior for the H_2O + CO_2 Mixture. *J. Phys. Chem. C* **2019**, *123*, 28123–28130.

(64) Vega, C.; Abascal, J. L.; Nezbeda, I. Vapor-Liquid Equilibria from the Triple Point Up to the Critical Point for the New Generation of TIP4P-Like Models: TIP4P/Ew, TIP4P/2005, and TIP4P/Ice. *J. Chem. Phys.* **2006**, *125*, 034503–1–034503–9.

(65) García-Fernández, R.; Abascal, J. L.; Vega, C. The Melting Point of Ice Ih for Common Water Models Calculated from Direct Coexistence of the Solid-Liquid Interface. *J. Chem. Phys.* **2006**, *124*, 144506–1–144506–11.

(66) Gloor, G. J.; Jackson, G.; Blas, F. J.; Miguel, E. D. Test-Area Simulation Method for the Direct Determination of the Interfacial Tension of Systems with Continuous or Discontinuous Potentials. *J. Chem. Phys.* **2005**, *123*, 134703/1–19.

(67) MacDowell, L. G.; Blas, F. J. Surface Tension of Fully Flexible Lennard-Jones Chains: Role of Long-Range Corrections. *J. Chem. Phys.* **2009**, *131*, 074705/1–10.

(68) Biscay, F.; Ghoufi, A.; Malfreyt, P. Surface Tension of Water-Alcohol Mixtures from Monte Carlo Simulations. *J. Phys. Chem. B* **2011**, *134*, 044709/1–10.

(69) Blas, F. J.; Moreno-Ventas Bravo, A. I.; Míguez, J. M.; Piñeiro, M. M.; MacDowell, L. G. Vapor-liquid Interfacial Properties of Rigid-Linear Lennard-Jones Chains. *J. Chem. Phys.* **2012**, *137*, 084706/1–11.

(70) Martínez-Ruiz, F. J.; Blas, F. J.; Mendiboure, B.; Moreno-Ventas Bravo, A. I. Effect of Dispersive Long-Range Corrections to the pressure Tensor: The Vapour-Liquid Interfacial Properties of the Lennard-Jones System Revisited. *J. Chem. Phys.* **2014**, *141*, 184701/1–17.

Graphical TOC Entry

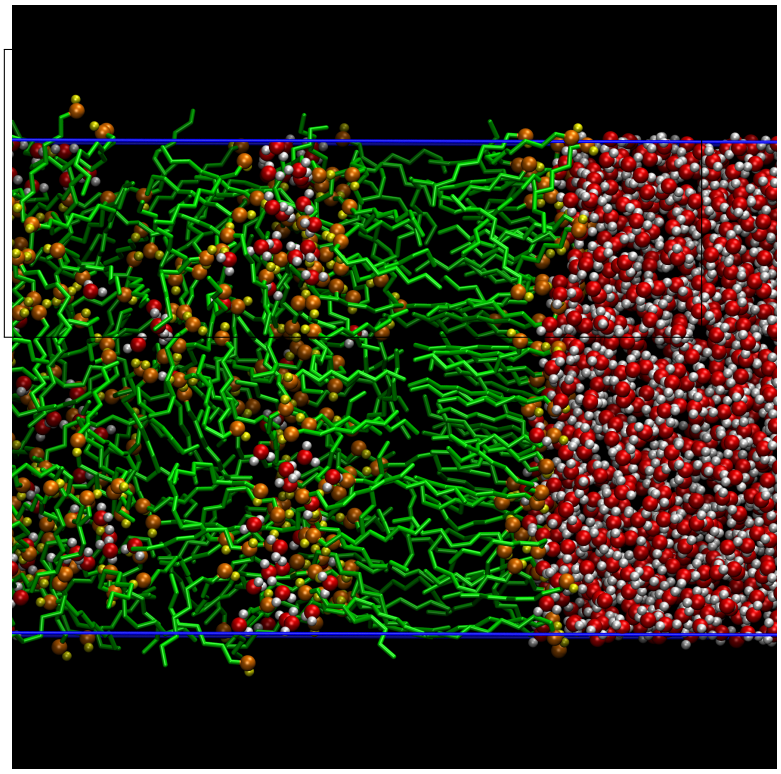

Snapshot of the liquid-liquid interface of the octan-1-ol + water mixture as obtained from molecular dynamics simulation